• Basic Research •

Desferrioxamine attenuating high glucose-induced ferroptosis and inflammatory responses in Müller glial cells *via* Nrf2/TXNRD1 pathway

Min Luo[1], *Yi Zhang*[1], *Na Li*[2], *Wen-Fang Zhan*[1]

[1]Department of Ophthalmology, Sanming First Hospital Affiliated to Fujian Medical University, Sanming 365000, Fujian Province, China

[2]Department of Ophthalmology, Ruijin Hospital, Affiliated Shanghai Jiao Tong University School of Medicine, Shanghai 200025, China

Co-first Authors: Min Luo and Yi Zhang

Correspondence to: Wen-Fang Zhan. Department of Ophthalmology, Sanming First Hospital Affiliated to Fujian Medical University, 29 Liedong Street, Sanming 365000, Fujian Province, China. zwf070820@163.com; Na Li. Department of Ophthalmology, Ruijin Hospital Affiliated Shanghai Jiao Tong University School of Medicine, 197 Ruijin Er Road, Shanghai 200025, China. ln11467@rjh.com.cn

Received: 2025-06-10 Accepted: 2026-02-04

Abstract

● **AIM:** To investigate the protective effects of deferoxamine (DFO) on high glucose (HG)-induced ferroptosis and inflammatory responses in retinal Müller glial cells (MGCs) and offer potential therapeutic targets for early intervention in diabetic retinopathy (DR).

● **METHODS:** Primary MGCs were cultured from C57BL/6J mouse retinas and exposed to normal glucose (NG, 5 mmol/L) or HG (25 mmol/L) conditions for various durations. Ferroptosis-related markers, including intracellular Fe^{2+} levels, glutathione (GSH), reactive oxygen species (ROS), malondialdehyde (MDA), and key proteins glutathione peroxidase 4 (GPX4), solute carrier family 7 member 11 (SLC7A11), ferritin heavy chain 1 (FTH1), were examined using multiple assays such as immunoblotting, enzyme-linked immunosorbent assay (ELISA), immunofluorescence (IF), and fluorometric detection. The role of DFO was evaluated through cell viability assessment and analysis of inflammatory cytokines interleukin-1 beta (IL-1β) and tumor necrosis factor-alpha (TNF-α).

● **RESULTS:** HG exposure significantly increased intracellular Fe^{2+} content, decreased GSH levels, elevated ROS and MDA concentrations, and altered expression profiles of ferroptosis regulators GPX4 and SLC7A11. Immunoblot and IF analyses confirmed downregulation of GPX4 and SLC7A11 alongside accumulation of FTH1 under prolonged HG treatment. DFO administration markedly attenuated these ferroptotic changes while reducing inflammatory cytokine secretion, demonstrating its protective effect against HG-induced damage in MGCs by modulating the nuclear factor erythroid 2-related factor 2 (Nrf2)/thioredoxin reductase 1 (TXNRD1) pathway.

● **CONCLUSION:** Low-dose DFO effectively mitigates HG-induced ferroptosis and inflammatory responses in MGCs through the Nrf2/TXNRD1 signaling axis, providing a theoretical framework for developing novel therapeutic strategies in DR management.

● **KEYWORDS:** ferroptosis; inflammatory; Müller cell; deferoxamine; diabetic retinopathy

DOI:10.18240/ijo.2026.09.05

Citation: Luo M, Zhang Y, Li N, Zhan WF. Desferrioxamine attenuating high glucose-induced ferroptosis and inflammatory responses in Müller glial cells *via* Nrf2/TXNRD1 pathway. *Int J Ophthalmol* 2026;19(9):1700-1710

INTRODUCTION

Diabetic retinopathy (DR) is one of the severe diabetes complexity. Globally, about one-third of diabetics develop retinopathy. DR can cause irreversible vision loss or blindness, becoming a primary cause of severe vision loss among working-age adults in high-income nations[1].

The pathogenesis of DR encompasses multifaceted pathophysiological mechanisms, initially characterized by neuroinflammatory responses, degenerative alterations, and Müller cell activation, ultimately culminating in microvascular impairment[2]. Contemporary therapeutic approaches, including anti-vascular endothelial growth factor (VEGF) pharmacotherapy and laser photocoagulation, predominantly target advanced pathological manifestations while demonstrating limited efficacy in early-stage intervention. As the principal glial cells in retinal, Müller glial cells (MGCs)

serve a vital function in maintaining blood-retinal barrier (BRB) integrity and retinal homeostasis through dynamic regulatory mechanisms[3]. Notably, hyperglycemic conditions induce pathological alterations in Müller cell functionality, manifesting as apoptotic processes, pro-inflammatory activation, and oxidative stress cascades. Experimental evidence from transgenic models with targeted Müller cell ablation demonstrates subsequent BRB disruption and pathological iron deposition, thereby substantiating their critical regulatory function in retinal iron metabolism[4]. Both *in vivo* diabetic models and *in vitro* high-glucose (HG) culture systems exhibit exacerbated ferroptotic within Müller cell populations[5-7].

Ferroptosis, a newly identified iron-regulated programmed cellular demise mechanism, has emerged as a critical mechanism in DR progression through lipid peroxidation cascade and glutathione (GSH) metabolism dysregulation[8-9]. Characteristic ultrastructural manifestations include mitochondrial condensation with elevated membrane density, cristae reduction, and outer membrane rupture[10]. The pathological triad of glutathione peroxidase 4 (GPX4) downregulation, iron homeostasis disruption, and intracellular lipid reactive oxygen species (ROS) accumulation constitutes primary ferroptosis drivers[11]. Notably, cerebral iron dysregulation induces neurodegeneration *via* oxidative stress and neuroinflammatory activation[12]. Experimental evidence demonstrates that ferroptosis inhibition in activated microglia attenuates neuroinflammatory responses[13]. In traumatic brain injury models, the iron-chelating agent deferoxamine (DFO) exhibits neuroprotective effects by suppressing ferroptosis mediated inflammation and improving neurological outcomes[14].

Hyperglycemia induced Müller cell activation in DR pathophysiology promotes interleukin-1 beta (IL-1β), tumor necrosis factor-alpha (TNF-α), and interleukin-6 (IL-6) secretion, establishing an inflammation-promoting retinal microenvironment that precipitates neuronal apoptosis and vascular dysfunction[15-16]. Elucidating the crosstalk between ferroptotic pathways and inflammatory cascades in MGCs represents a crucial therapeutic target for early DR intervention. The Nrf2 emerges as a pivotal controller at the ferroptosis-neuroinflammation interface[17]. Mechanistically, Nrf2 modulates ferroptosis related proteins expression through direct binding to antioxidant response elements (AREs) in the thioredoxin reductase 1 (TXNRD1) gene promoter[18]. These findings collectively underscore the Nrf2/TXNRD1 signaling axis as a master regulator of ferroptosis and neuroinflammatory processes in DR pathogenesis.

DFO, a clinically approved iron-chelating agent, has been extensively employed in both therapeutic and analytical applications. The U.S. Food and Drug Administration (FDA) has granted approval for its usage for managing chronic iron overload in hematological encompass conditions such as thalassemia, sickle cell anemia, and myelodysplastic disorders[19]. Experimental evidence from multiple animal models demonstrates DFO's neuroprotective efficacy: in adult rat models, it effectively mitigates oxidative damage through iron chelation-mediated attenuation of neuronal ferroptosis[20], while also promoting rehabilitation following severe spinal cord trauma *via* ferroptosis inhibition[21]. Remarkably, subclinical doses (3–80 times below therapeutic levels) exhibit neuroprotective properties exhibiting protective effects against retinal injury induced by N-methyl-D-aspartate (NMDA) in rodents[22]. Furthermore, Zn/DFO co-treatment significantly ameliorates degenerative retinal pathology in the rd10 mouse model of retinal degeneration[23]. Despite these advances, the molecular mechanisms underlying DFO's regulation of HG induced ferroptosis and inflammatory responses in MGCs remain unexplored.

Through *in vitro* simulation of DR pathophysiology using hyperglycemic conditions, this investigation elucidates that low-dose DFO modulates MGCs ferroptosis and inflammatory processes under hyperglycemic stress *via* the Nrf2/TXNRD1 signaling axis. These results establish a theoretical framework and experimental basis for identifying novel therapeutic targets in DR pharmacotherapy development.

MATERIALS AND METHODS

Ethical Approval Each experimental procedure was conducted in compliance with the Association for Research in Vision and Ophthalmology (ARVO) Statement regarding animal use in ophthalmic research and adhered to the regulations set forth by the Ethics Committee of Sanming First Hospital Affiliated to Fujian Medical University, China (Protocol #2024-106). We reduced the quantity of animals involved and alleviated their distress throughout the experimental procedures.

Cell Culture and HG Intervention Primary retinal MGCs were dissociated from C57BL/6J mouse retinas and maintained in appropriate growth medium using established protocols[24]. Cell cultures were maintained in Dulbecco's modified Eagle's medium (DMEM, Gibco, NY, USA) cultured in medium containing 10% fetal bovine serum (FBS) and incubated at 37°C under a humidified atmosphere of 5% CO_2 and 95% air. For glucose treatments, normal glucose (NG) and HG conditions were established by growing cells in DMEM containing 5 mmol/L or 25 mmol/L D-glucose respectively during 0–24h incubations. In the experiments using the ferroptosis and Nrf2 inhibitors, MGCs underwent DFO treatment and 5 μmol/L ML385 for 24h[25].

Immunoblot Cells were lysed with radio-immunoprecipitation assay (RIPA) buffer (Beyotime Biotechnology, Shanghai,

China) supplemented with protease inhibitor additives and Phenylmethanesulfonyl fluoride (PMSF). Following extensive centrifugation at 12 000×g, the resultant supernatants were harvested for protein quantification using a BCA protein assay kit (P0009, Beyotime, China). Subsequently, protein specimens were electrophoresed on 10% sodium dodecyl sulfate-polyacrylamide gel (SDS-PAGE) and subsequently transferred onto polyvinylidene difluoride (PVDF) membranes (0.45 μm pore size; Millipore, USA). The membranes underwent blocking using 5% non-fat milk in tris-buffered saline (TBS) with 0.1% Tween-20 (TBST) for 2h, comes after overnight incubation with specific primary antibodies at 4°C. After TBST washing cycles, membranes were probed with horseradish peroxidase (HRP)-conjugated secondary antibodies (7074S, Cell Signaling Technology, USA, 1:1000) for 90min at room temperature. Protein signals were crafted *via* enhanced chemiluminescence (ECL) substrate (Thermo Fisher Scientific, USA) and quantitatively analyzed through densitometry with ImageJ 6.0 software. The following primary antibodies were utilized: β-actin (ab179467, Abcam, UK, 1:5000), GPX4 (A11243, Abclonal, China, 1:1000), solute carrier family 7 member 11 (SLC7A11; A13685, Abclonal, China, 1:1000), ferritin heavy chain 1 (FTH1; A19544, Abclonal, China, 1:1000), IL-1β (12426, Cell Signaling Technology, USA, 1:1000), TNF-α (11948, Cell Signaling Technology, USA, 1:1000), Nrf2 (A0674, Abclonal, China, 1:1000), TXNRD1 (ab124954, Abcam, UK, 1:10000).

Enzyme-Linked Immunosorbent Assay MGCs were seeded in 12-well plates and cultured until reaching 80% confluence. Following experimental treatments, the medium was gathered and centrifuged at 1500 rpm for 5min to form granular cell fragments. The resulting supernatant was subsequently analyzed for cytokine levels using commercial mouse enzyme-linked immunosorbent assay (ELISA) kits (IL-1β: MEC1010, Anogen, Canada; TNF-α: MEC1003, Anogen, Canada) following the manufacturer's protocols.

Immunofluorescence Cell climbing slices were immobilized with 4% paraformaldehyde at ambient temperature for 10min，subsequently incubated in 0.5% Triton X-100 solution at 37°C for 5min. After three phosphate buffered saline (PBS) washes (10min each), The samples were blocked using 10% buck serum, followed by an overnight incubation at 4°C with primary antibodies targeting: GPX4 (A11243, Abclonal, China, 1:200), SLC7A11 (ab307601, Abcam, USA, 1:500), FTH1 (A19544, Abclonal, China, 1:200). Following the washing away of primary antibodies，the cells were treated with secondary antibodies at 37°C for 60min: Alexa Fluor™ Plus 555-conjugated anti-rabbit IgG (A32732, Thermo Fisher Scientific, USA), followed by washing. The nuclei were stained with 4',6-diamidino-2-phenylindole (DAPI; C1006, Beyotime, China) for 10min, followed by 3 washes (10min each). Cell examination and image acquisition were performed utilizing fluorescence microscopy (Nikon Eclipse Ts2).

Ferrous Iron Detection Intracellular Fe^{2+} levels were measured using the Cell Ferrous Iron (Fe^{2+}) Fluorometric Assay Kit (MA0647, Meilun, China) following the manufacturer's protocol. Cells were treated with 1 μmol/L staining solution in culture medium for 30min at 37°C under 5% CO_2 conditions. Fluorescence imaging was conducted within 2h using a Nikon fluorescent microscope for cellular observation and documentation.

ROS Detection The intracellular ROS levels were measured using a Reactive Oxygen Species Assay Kit (S0033S, Beyotime Biotechnology, Shanghai, China). Briefly, the cells were incubated in medium containing 10 μmol/L DCFH-DA for 20min at 37°C and then the cells were observed and the images were captured under a fluorescent microscope (Nikon) within 2h.

GSH and MDA Assay Intracellular GSH levels and malondialdehyde (MDA) concentrations were analyzed using commercial assay kits (GSH: S0052; MDA: S0131S, both from Beyotime Biotechnology, Shanghai, China). Following cell collection and homogenization, samples underwent centrifugation at 10 000×g for 10min under 4°C conditions. The resultant supernatants were subsequently processed according to standardized protocols provided with each detection kit. Spectrophotometric measurements were conducted at specific wavelengths: 412 nm for GSH quantification and 532 nm for MDA analysis. Protein concentrations in experimental samples were concurrently determined using a BCA protein assay system to ensure measurement standardization.

Cell Viability Assay Cell counting kit-8 (CCK-8) assay (C0037, Beyotime, China) was employed to assess MGCs viability following the supplier's instructions. Briefly, MGCs were plated in 96-well culture dishes at a density of 8×10^3 cells/well. After 24h incubation under standard conditions, the cells underwent various experimental treatments. Subsequently, 20 μL of CCK-8 reagent was directly introduced into each well, followed by a 2h incubation period at 37°C. Absorbance measurements were then conducted using a microplate reader set to 450 nm wavelength.

Statistical Analysis Experimental results are presented as mean±standard deviation (SD) derived from at least three independent replicates. Statistical evaluations between two groups were conducted using two-tailed Student's *t*-tests, whereas multi-group comparisons employed one-way analysis of variance (ANOVA) with Tukey's post hoc analysis. All analyses were performed through GraphPad Prism 8.1.1 (GraphPad Software, Inc.), with $P<0.05$ serving as the threshold for statistical significance.

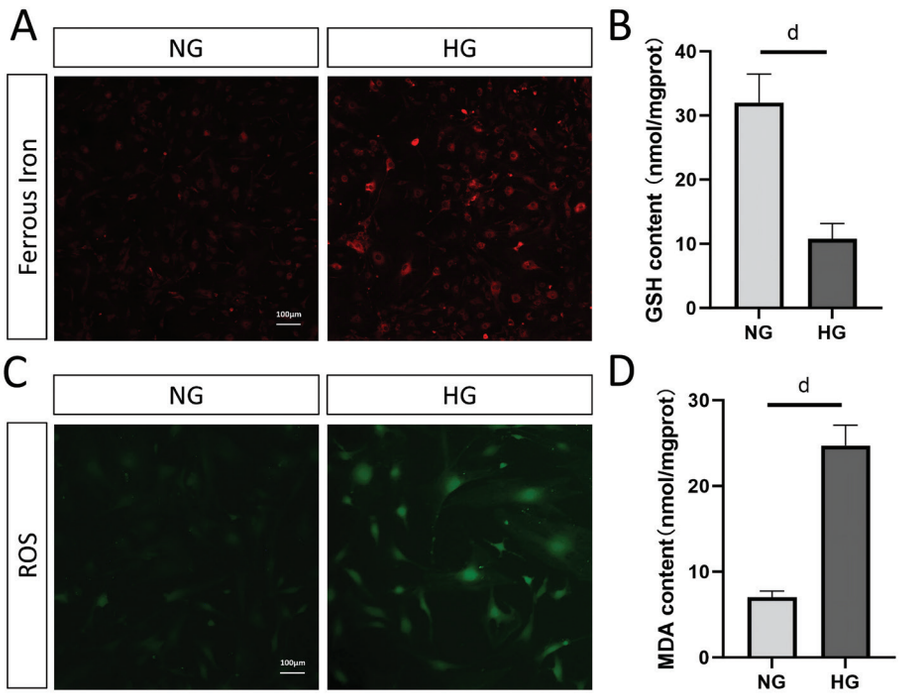

Figure 1 HG induces changes in iron level, GSH concentration, ROS level, and MDA content in MGCs A: Ferrous ion level was remarkably increased in HG stimulated MGCs compared with the NG culture cells; B: HG induced a marked decrease in GSH concentration after 24h; C: Cell ROS level revealed an increase in HG stimulated MGCs after 24h; D: HG caused an obvious increase in MDA content in MGCs after 24h. $^{d}P<0.0001$ versus NG groups. Scale bar: 100 μm. HG: High glucose; GSH: Glutathione; ROS: Reactive oxygen species; MDA: Malondialdehyde; MGCs: Müller glial cells; NG: Normal glucose.

RESULTS

HG Promotes Ferroptosis in MGCs To determine whether HG environment induce ferroptosis in MGCs, researchers exposed the cells to 25 mmol/L glucose-enriched culture medium for 24h. Intracellular ferrous ion (Fe^{2+}) detection revealed a marked increase in Fe^{2+} content under HG conditions (Figure 1A). The stimulated MGCs exhibited a striking metabolic imbalance: GSH levels plummeted (Figure 1B) while lipid peroxidation products surged significantly, as evidenced by elevated MDA concentrations (Figure 1D). Simultaneously, elevated levels of ROS were detected in MGCs subjected to HG treatment (Figure 1C). Subsequent experimental analyses demonstrated that chronological exposure to HG induced time-dependent upregulation of the iron metabolism regulator FTH1. Notably, the expression profiles of key ferroptosis regulators GPX4 and SLC7A11 exhibited transient elevation during the initial phases of hyperglycemic stimulation (6h and 12h), followed by significant attenuation upon prolonged exposure (24h) as evidenced by immunoblotting results (Figure 2A). Complementary immunofluorescence (IF) assays corroborated these findings, revealing substantial downregulation of GPX4 and SLC7A11 protein levels in MGCs following 24h HG treatment (Figures 2C, 2D), while concurrently demonstrating pronounced accumulation of FTH1 (Figure 2B).

HG Triggers the Expression of Cytokine in MGCs Subsequently, we investigated the cytokine expression of MGCs under hyperglycemic conditions (24h exposure). Western blot revealed significant upregulation of both IL-1β and TNF-α protein levels compared to control groups (Figure 3A). Correspondingly, ELISA measurements of cell culture supernatants demonstrated a time-dependent elevation in secreted IL-1β (Figure 3B) and TNF-α (Figure 3C) protein concentrations under sustained HG conditions.

DFO Alleviates HG Induced MGCs Cytokine Expression and Inhibiting Ferroptosis We subsequently examined the DFO on HG-induced ferroptosis and inflammatory responses in MGCs. Dose-response experiments demonstrated that 20 μmol/L DFO effectively reduced IL-1β and TNF-α expression in HG stimulated MGCs, while 100 μmol/L elevated TNF-α beyond control levels (Figure 4A). The optimal 20 μmol/L concentration decreased intracellular Fe^{2+} and ROS accumulation (Figure 4B), concurrently suppressing lipid peroxidation evidenced by reduced MDA levels (Figure 4C) and enhancing antioxidant capacity through GSH elevation (Figure 4D). Immunoblotting revealed that low-dose DFO differentially regulated ferroptosis markers: downregulating FTH1 while upregulating GPX4 and SLC7A11 in glucose-stressed MGCs (Figure 5A). IF corroborated these protein expression changes, showing increased GPX4/SLC7A11 fluorescence intensity (Figures 5C, 5D) and reduced FTH1 signals (Figure 5B), achieving complete consistency with Western blot results.

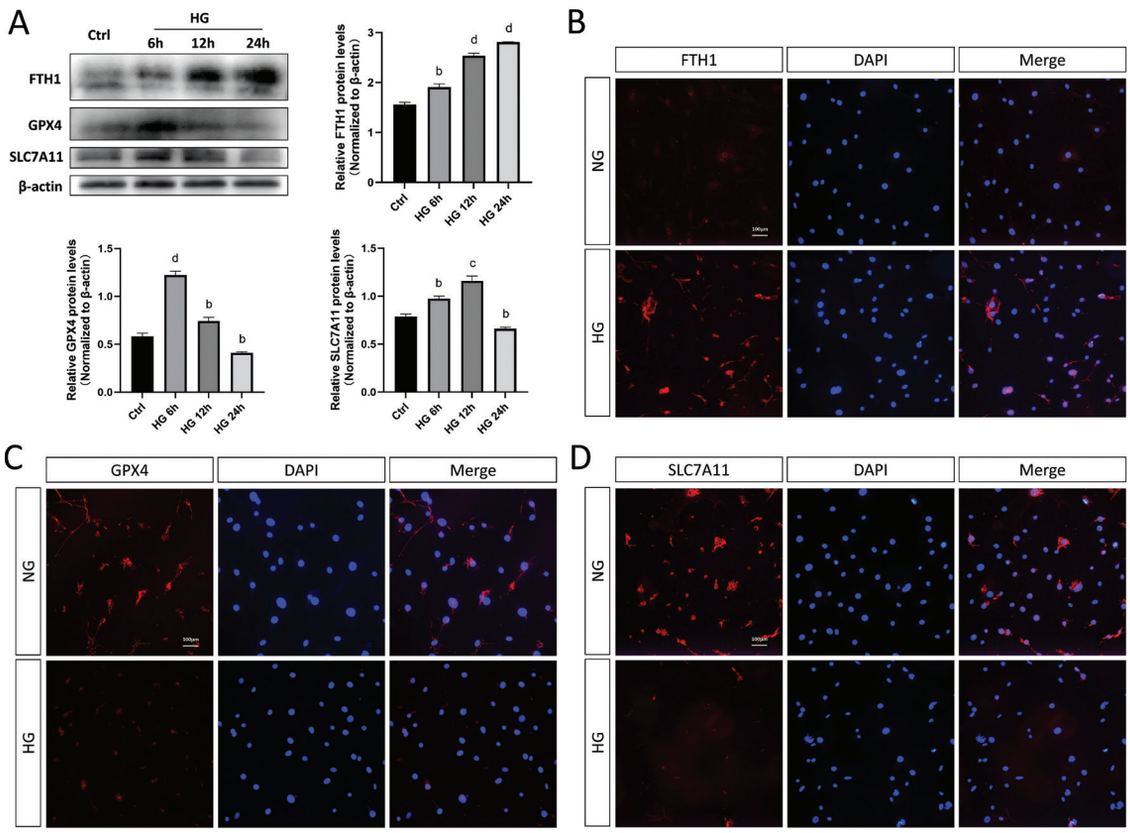

Figure 2 HG causes changes in the expression of ferroptosis-related proteins in MGCs A: Western blot analysis of ferroptosis-related protein expression levels in HG stimulated MGCs. β-actin was used as an internal control in analysis. HG induced obvious upregulation in the expression of FTH1 in MGCs compared with the Ctrl groups. Expression of GPX4 and SLC7A11 proteins was significantly upregulated in HG stimulated MGCs after 6, 12h, and downregulated after 24h. B–D: IF staining of localization of ferroptosis-related proteins (red) and nuclear (blue) in HG stimulated MGCs after 24h. Data are shown as mean±SD, n=6 per group for Western blotting. ^{b}P<0.01, ^{c}P<0.001, ^{d}P<0.0001 versus Ctrl groups. Scale bar: 100 μm. HG: High glucose; MGCs: Müller glial cells; FTH1: Ferritin heavy chain 1; GPX4: Glutathione peroxidase 4; SLC7A11: Solute carrier family 7 member 11; IF: Immunofluorescence; SD: Standard deviation; NG: Normal glucose; DAPI: 4′,6-diamidino-2-phenylindole.

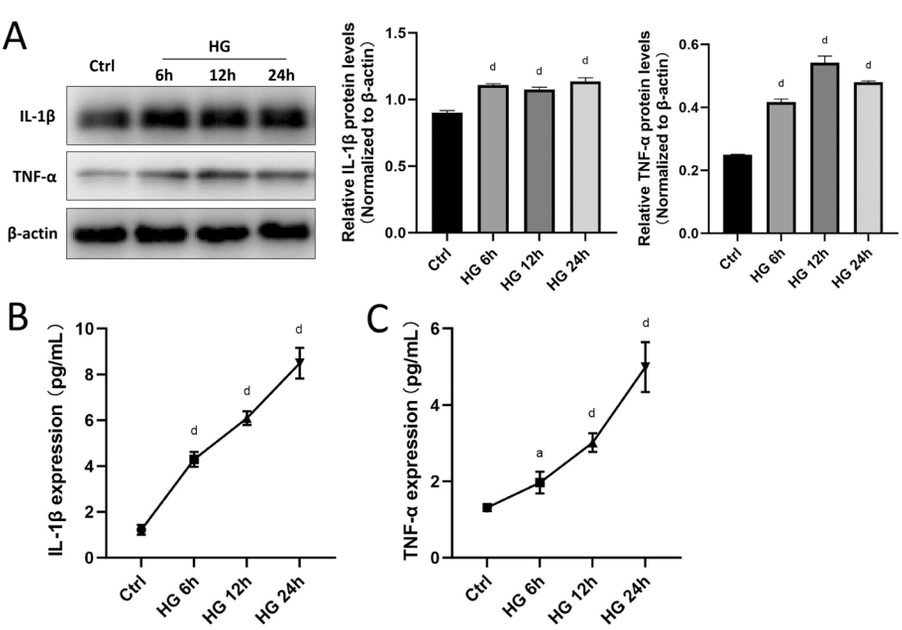

Figure 3 HG causes changes in the expression of IL-1β and TNF-α in MGCs A: Western blot analysis demonstrated that the protein expression levels of IL-1β and TNF-α in HG stimulated MGCs were significantly elevated compared to the Ctrl groups. β-actin was used as an internal control in analysis. B, C: IL-1β and TNF-α concentrations in MGCs culture supernatants were quantified using ELISA. Data are shown as mean±SD, n=6 per group for Western blotting. ^{a}P<0.05, ^{d}P<0.0001 *vs* Ctrl groups. HG: High glucose; MGCs: Müller glial cells; IL-1β: Interleukin-1 beta; TNF-α: Tumor necrosis factor-alpha; ELISA: Enzyme-linked immunosorbent assay; SD: Standard deviation.

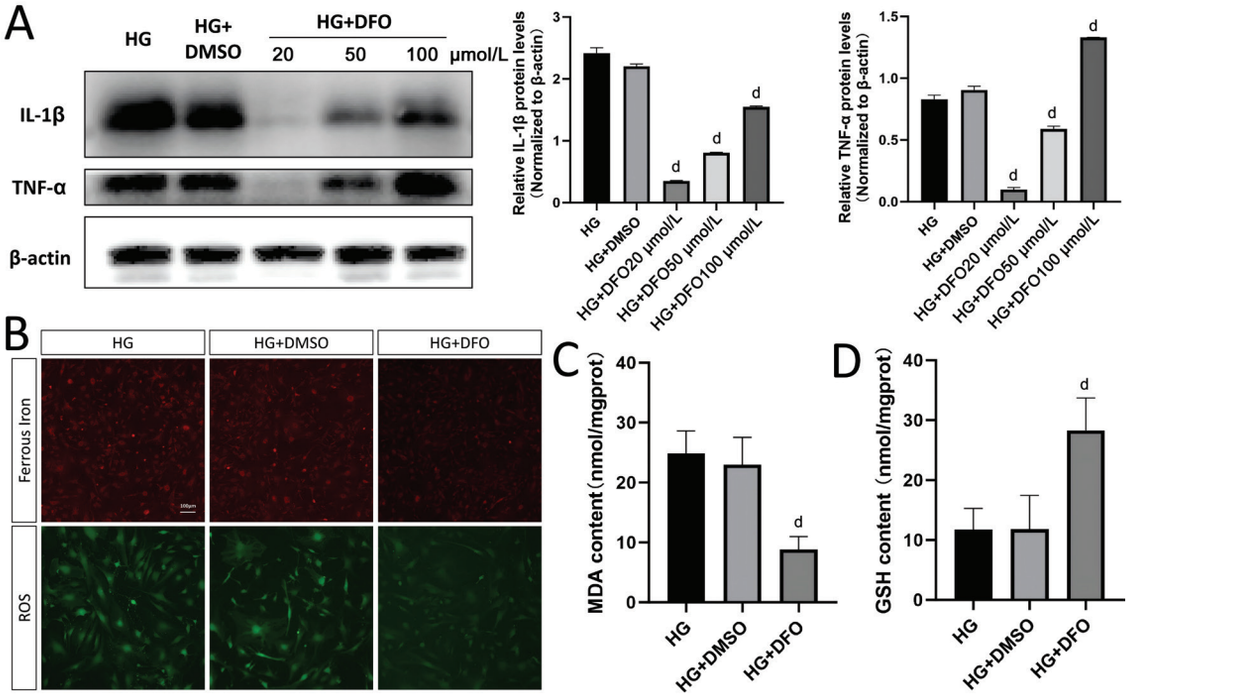

Figure 4 DFO administration reduced IL-1β and TNF-α protein expression changes and altered iron levels, GSH, ROS, and MDA content in HG stimulated MGCs A: Western blot analysis of IL-1β and TNF-α proteins expression levels in HG cultured MGCs after DFO treatment. β-actin was used as an internal control. The expression of IL-1β and TNF-α protein expression was markedly attenuated following 20 μmol/L DFO treatment, but rebounded at higher concentrations of 50/100 μmol/L DFO. B: Ferrous ion and ROS level was remarkably decreased after DFO treatment in HG stimulated MGCs. C: DFO treatment induced a marked decrease of MDA content in HG induced MGCs. D: DFO treatment caused an obvious increase in GSH concentration. Data are shown as mean±SD, n=6 per group for Western blotting. ^{d}P<0.0001 *vs* HG groups. Scale bar: 100 μm. DFO: Deferoxamine; IL-1β: Interleukin-1 beta; TNF-α: Tumor necrosis factor-alpha; HG: High glucose; MGCs: Müller glial cells; ROS: Reactive oxygen species; MDA: Malondialdehyde; GSH: Glutathione; SD: Standard deviation; DMSO: Dimethyl sulfoxide.

DFO Inhibited the Ferroptosis and Cytokine Expression of MGCs *via* Nrf2/TXNRD1 Pathway Finally, we investigated whether the Nrf2/TXNRD1 pathway proteins play a critical role in DFO's effect on HG-induced ferroptosis in MGCs. First, Western blot analysis revealed that HG conditions significantly reduced the protein levels of Nrf2 and TXNRD1, whereas treatment with DFO restored their protein levels (Figure 6A), indicating that DFO can activate the Nrf2/TXNRD1 pathway under HG conditions. Moreover, CCK-8 assay results demonstrated that DFO partially restored HG induced the inhibition of cell viability, and without affecting cellular activity under NG conditions (Figure 6B). To further validate the role of Nrf2 pathway, MGCs were treated with DFO and the Nrf2 pathway inhibitor ML385 (5 μmol/L, 24h). Western blot results demonstrated that ML385 significantly decreased the protein expression of Nrf2 and its downstream target TXNRD1. It concurrently lowered GPX4 and SLC7A11 levels while upregulating FTH1 expression. Additionally, ML385 enhanced the levels of IL-1β and TNF-α cytokines (Figure 7A). Statistical evaluation demonstrated that all observed changes exhibited significant differences (Figure 7B).

DISCUSSION

The research findings reveal that the HG environment induce ferroptosis in MGCs and amplifies inflammatory factors expression. Notably, low-dose DFO suppresses both ferroptosis and inflammatory responses in MGCs under hyperglycemic condition, mediated by the activation of Nrf2/TXNRD1 pathway. The results provide a new idea for DR therapy: low-dose DFO demonstrates promising therapeutic potential in targeting ferroptosis driven inflammation within MGCs.

During the pathological progression of DR, mitochondrial dysfunction and oxidative stress cascades promote the transformation of Müller cells into a pathologically activated state, characterized by a gliotic response with significant upregulation of glial fibrillary acidic protein (GFAP) expression. Our previous studies confirmed that after 24h of HG culture *in vitro*, Müller cells displayed high expression of GFAP and pro-inflammatory cytokines (IL-1β, TNF-α)[24]. Proteomic analysis of aqueous humor in patients with proliferative DR demonstrated that ferroptosis-related proteins are strongly associated with immune responses, stress responses, and cellular metabolism[26]. Recent studies indicate that ferroptosis of Müller cells plays a crucial regulatory role in retinal microenvironment homeostasis. MGCs established a metabolic buffer zone between the retinal pigment epithelium and photoreceptors through an iron-

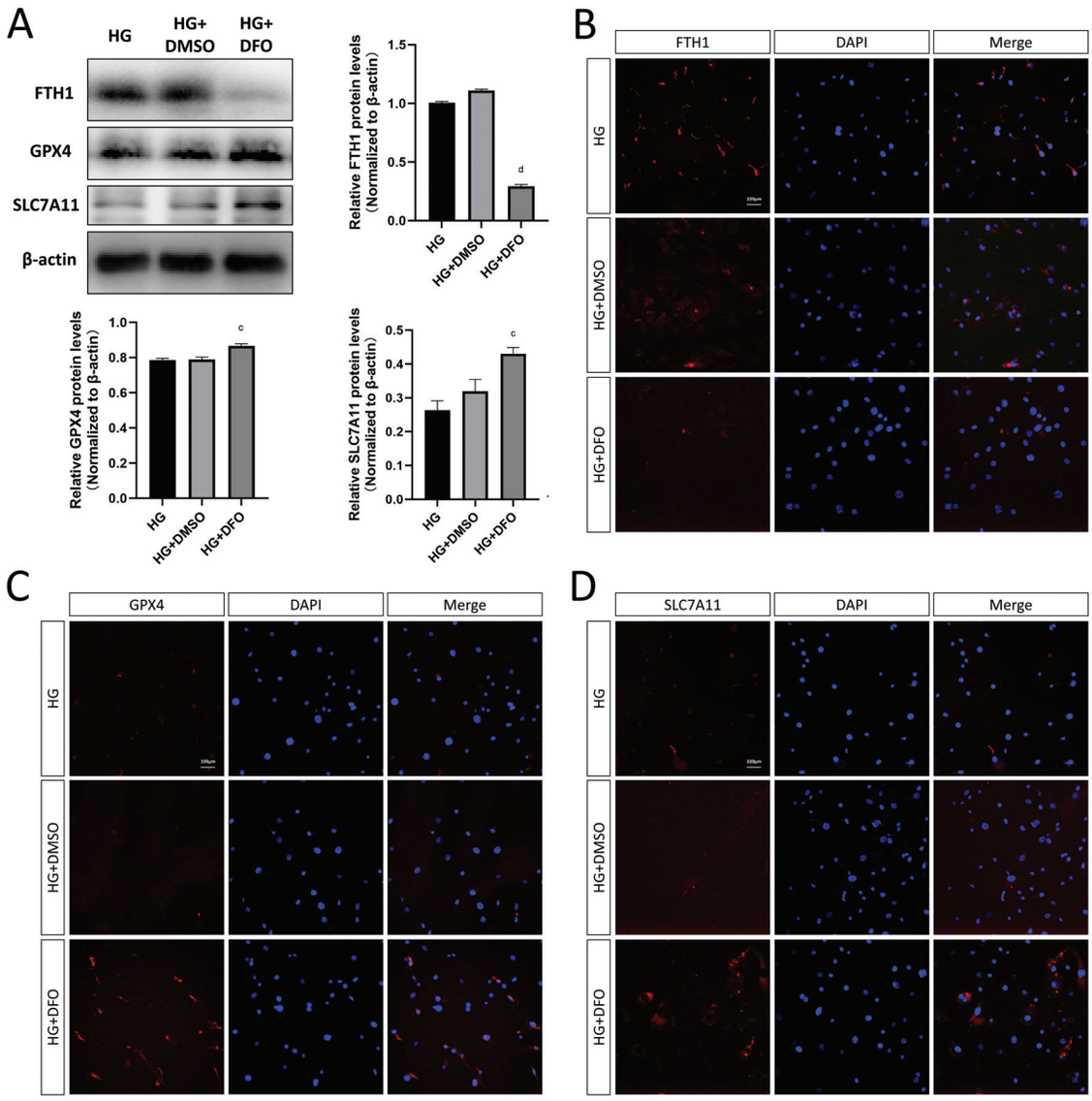

Figure 5 DFO administration altered ferroptosis-related proteins in HG stimulated MGCs A: Western blot analysis of ferroptosis-related proteins expression levels in HG-induced MGCs after DFO treatment. β-actin was used as an internal control. The expression of FTH1 was markedly attenuated following DFO treatment, and DFO treatment induced obvious upregulation in the expressions of GPX4 and SLC7A11 proteins. B–D: IF staining of the localization of ferroptosis-related proteins (red) and nuclear (blue) in HG-induced MGCs after DFO treatment. Data are shown as mean±SD, n=6 per group for Western blotting. ^{c}P<0.001, ^{d}P<0.0001 *vs* HG groups. Scale bar: 100 μm. DFO: Deferoxamine; HG: High glucose; MGCs: Müller glial cells; FTH1: Ferritin heavy chain 1; GPX4: Glutathione peroxidase 4; SLC7A11: Solute carrier family 7 member 11; IF: Immunofluorescence; SD: Standard deviation; DAPI: 4',6-diamidino-2-phenylindole; DMSO: Dimethyl sulfoxide.

dependent lipid peroxidation mechanism. Its programmed cell death process can lead to GSH metabolic cycle disorders and trigger abnormal mitochondrial membrane potential in inner retinal neurons[27-28]. However, the molecular regulatory mechanisms between retinal Müller cell ferroptosis and the pro-inflammatory cytokine network under HG stress conditions still lack systematic investigation.

DFO, as an iron chelator, demonstrates regulatory effects on neuronal ferroptosis in the central nervous system (CNS). Its molecular mechanisms involve inhibition of lipid peroxidation and modulation of the Nrf2 signaling pathway[29-30]. Previous research has established that activating the Nrf2/HO-1 pathway inhibits ferroptosis, thus protecting retinal microvascular endothelial cells (RMECs) from HG-induced damage[31]. In lipopolysaccharide-induced cognitive impairment models, DFO significantly reduces hippocampal IL-6 and TNF-α levels while ameliorating microglial overactivation by suppressing abnormal iron accumulation and regulating the homeostasis of iron metabolism-related protein expression[32]. Additionally, it markedly improves amyloid-β deposition and cognitive dysfunction, potentially through modulating the pro-inflammatory phenotypic transformation of microglia[33].

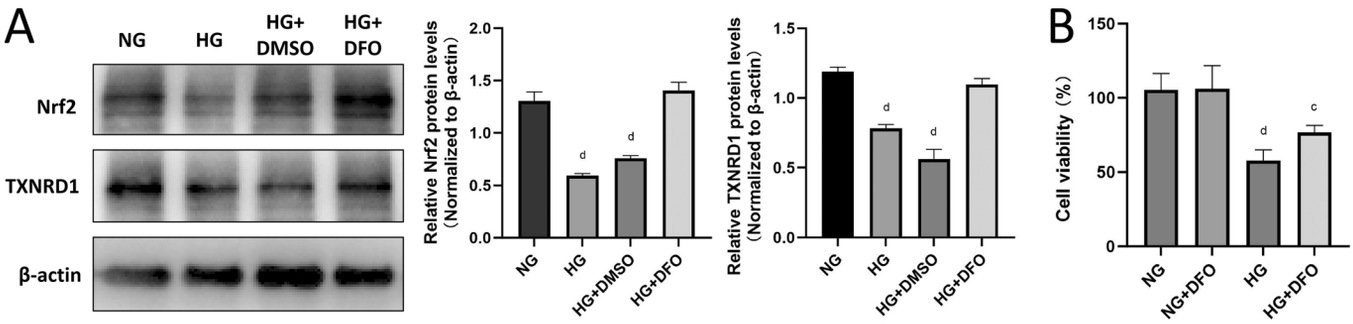

Figure 6 DFO treatment modulated Nrf2/TXNRD1 protein expression in HG-induced MGCs without affecting cell viability A: Western blot analysis demonstrated that DFO treatment effectively restored the HG-induced reduction in Nrf2 and TXNRD1 protein expression levels. β-actin was used as an internal control. B: CCK-8 assay showed DFO reversed HG-induced cell viability inhibition, and without affecting activity under NG condition. Data are shown as mean±SD, n=6 per group for Western blotting. ^{c}P<0.001, ^{d}P<0.0001 *vs* NG groups. DFO: Deferoxamine; Nrf2: Nuclear factor erythroid 2-related factor 2; TXNRD1: Thioredoxin reductase 1; HG: High glucose; MGCs: Müller glial cells; CCK-8: Cell Counting Kit-8; NG: Normal glucose; SD: Standard deviation.

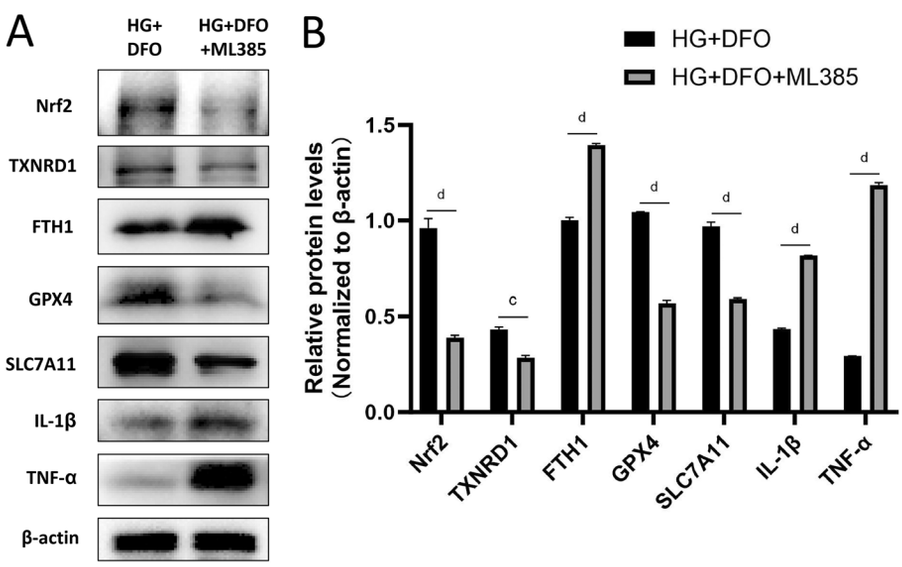

Figure 7 DFO alleviated ferroptosis and inflammatory responses in HG-induced MGCs by activating the Nrf2/TXNRD1 axis A: Western blot revealed ML385 (Nrf2 inhibitor) downregulated Nrf2 and TXNRD1 protein levels, reduced GPX4 and SLC7A11 expression, increased FTH1, and elevated IL-1β and TNF-α levels. β-actin was used as an internal control. B: Statistical analysis confirmed that all these results were significantly different. Data are shown as mean±SD, n=6 per group for Western blotting. ^{c}P<0.001, ^{d}P<0.0001 *vs* HG+DFO groups. DFO: Deferoxamine; HG: High glucose; MGCs: Müller glial cells; Nrf2: Nuclear factor erythroid 2-related factor 2; TXNRD1: Thioredoxin reductase 1; ML385: Nrf2 specific inhibitor; GPX4: Glutathione peroxidase 4; SLC7A11: Solute carrier family 7 member 11; FTH1: Ferritin heavy chain 1; IL-1β: Interleukin-1 beta; TNF-α: Tumor necrosis factor-alpha; SD: Standard deviation.

The research revealed for the first time that low-dose DFO treatment under *in vitro* conditions reverses the suppressed expression of ferroptosis-regulating proteins (GPX4, SLC7A11) in mouse Müller cells exposed to hyperglycemia, significantly reduce intracellular ROS and ferrous ion levels, decrease MDA levels while increasing GSH levels, and simultaneously suppress the expression of HG-induced inflammatory factors. ROS accumulation is a key mechanism driving ferroptosis. ROS triggers lipid peroxidation in phospholipid-rich cell membranes, generating MDA that directly induces cytotoxic effects and subsequently activates ferroptosis[34]. The reduction of ROS levels is a critical step in inhibiting ferroptosis in Müller cells. However, it is noteworthy that experimental data revealed the dual regulatory properties of DFO on ferroptosis markers: while enhancing the GPX4/SLC7A11 signaling axis, it suppresses the expression of FTH1. As a critical component of mammalian antioxidant defenses, GPX4 stands out as the sole enzyme identified to date that catalyzes the conversion of phospholipids into hydrogen peroxide[35]. Functioning as a crucial component in ferroptosis, SLC7A11 facilitates cystine uptake into cellular environments and catalyzes its conversion to cysteine[36]. Therefore, the restoration of SLC7A11 expression can promote GSH synthesis and enhance GPX4 activity, ultimately inhibiting

lipid peroxidation and maintaining the integrity of the cytoplasmic membrane, which serves a critical function in the morphology and function of Müller cells under HG condition. The regulation of ferritin expression is chiefly controlled by iron regulatory protein (IRP)-1 and IRP-2. Specifically, IRP-2 attaches to iron-responsive elements located in the 5' untranslated regions of both H- and L-ferritin mRNA strands, effectively suppressing their translation process. DFO treatment may inhibit the release of IRP-2 binding, thereby suppressing FTH1 expression[37-38], which could explain the observed decrease in FTH1 protein expression after DFO treatment.

Moreover, studies have demonstrated that TXNRD1 serves as a downstream target of Nrf2 and undergoes positive regulation by this transcription factor[39]. TXNRD1 plays a vital role in antioxidant responses[40]. Experimental data demonstrated the Nrf2-mediated upregulation of TXNRD1 in MGC. Pharmacological activation of the Nrf2/TXNRD1 axis through DFO administration was observed, while Nrf2 pathway blockade counteracted the suppressive effects of DFO on both ferroptotic processes and inflammatory activation in hyperglycemic-exposed Müller cells, concurrently diminishing TXNRD1 expression levels. TXNRD1 is plays a vital role in the thioredoxin (TXN) system and plays a crucial role in maintaining cellular redox balance and regulating various pathophysiological processes. TXNRD1 can reduce oxidized TXN, thereby counteracting the inhibitory binding effect of thioredoxin-interacting protein (TXNIP)[41]. Inhibition of the TXNIP/NLRP3 inflammasome pathway has shown potential in reducing DR-related inflammation and retinal damage[42-43].

The study proposes that DFO treatments at 50 and 100 μmol/L concentrations may intensify inflammatory responses through hypoxia-inducible factor-1 alpha (HIF-1α) mediated metabolic reprogramming mechanisms. High concentrations of DFO inhibit prolyl hydroxylase domain (PHD) enzymes, reducing the hydroxylation and degradation of HIF-1α and promoting its accumulation[44]. HIF-1α is a key metabolic reprogrammer in inflammatory cells and can promote the expression of inflammatory genes, particularly IL-1β[45]. These results indicate the presence of a dose-responsive control mechanism within the iron homeostasis-inflammatory response network, though its precise molecular pathways still need additional exploration.

In vitro findings reveal that low-concentration DFO effectively suppresses HG-induced ferroptosis and inflammatory responses in Müller cells through activation of the Nrf2/TXNRD1 signaling pathway. The current research foundation in this field remains relatively weak, highlighting the innovative value of this study. It should be noted that the regulatory networks of ferroptosis and inflammatory responses exhibit high complexity. Follow-up research plans to systematically investigate the biological effects of DFO in *in vivo* models, with a focus on analyzing its pharmacokinetic characteristics and the balance mechanism between efficacy and safety, thereby providing theoretical support and experimental evidence for clinical treatment strategies of DR.

ACKNOWLEDGEMENTS

Authors' Contributions: Luo M: Software, methodology, validation, data curation, funding acquisition. Zhang Y: Conceptualization, methodology, validation, writing–original draft, writing–review & editing. Li N: Conceptualization, methodology, validation, writing–review & editing, project administration. Zhan WF: Resources, supervision, project administration, funding acquisition. All the authors read and approved the final manuscript.

Data Availability Statement: The data that support the findings of this study are available on reasonable request from the corresponding author.

AI-Generated Content Disclosure: The language polishing of this content were assisted by WPS AI tools. We ensuring that the core viewpoints and professional judgments of the content are all human-led. We have conducted strict reviews and verifications of the AI-generated content to ensure compliance with relevant norms and requirements.

Foundation: Supported by Sanming Joint Funding Program in the Healthcare Sector (No.2024-S-082).

Conflicts of Interest: Luo M, None; **Zhang Y,** None; **Li N,** None; **Zhan WF,** None.

REFERENCES

1 Hendrick AM, Gibson MV, Kulshreshtha A. Diabetic retinopathy. *Prim Care* 2015;42(3):451-464.

2 Midena E, Pilotto E. Emerging insights into pathogenesis. *Dev Ophthalmol* 2017;60:16-27.

3 Carpi-Santos R, de Melo Reis RA, Gomes FCA, *et al*. Contribution of müller cells in the diabetic retinopathy development: focus on oxidative stress and inflammation. *Antioxidants* 2022;11(4):617.

4 Baumann B, Sterling J, Song Y, *et al*. Conditional müller cell ablation leads to retinal iron accumulation. *Invest Ophthalmol Vis Sci* 2017;58(10):4223-4234.

5 Dai RF, Qian Y, Liu SQ, *et al*. Growth arrest-specific 1 inhibits Keap1/Nrf2 signaling transduction in the activation of the ferroptosis program in retinal müller cells. *Front Biosci* (*Landmark Ed*) 2025;30(3):27954.

6 Wang Y, Song SY, Song Y, *et al*. Resveratrol protects müller cells against ferroptosis in the early stage of diabetic retinopathy by regulating the Nrf2/GPx4/PTGS2 pathway. *Mol Neurobiol* 2025;62(3):3412-3427.

7 Chen Z, Liu BJ, Zhou DJ, *et al*. AQP4 regulates ferroptosis and oxidative stress of Muller cells in diabetic retinopathy by regulating TRPV4. *Exp Cell Res* 2024;439(1):114087.

8 Li LX, Dai YC, Ke D, *et al*. Ferroptosis: new insight into the mechanisms of diabetic nephropathy and retinopathy. *Front Endocrinol (Lausanne)* 2023;14:1215292.

9 Jiang XJ, Stockwell BR, Conrad M. Ferroptosis: mechanisms, biology and role in disease. *Nat Rev Mol Cell Biol* 2021;22(4):266-282.

10 Xie Y, Hou W, Song X, *et al*. Ferroptosis: process and function. *Cell Death Differ* 2016;23(3):369-379.

11 Ursini F, Maiorino M. Lipid peroxidation and ferroptosis: The role of GSH and GPx4. *Free Radic Biol Med* 2020;152:175-185.

12 Ward RJ, Zucca FA, Duyn JH, *et al*. The role of iron in brain ageing and neurodegenerative disorders. *Lancet Neurol* 2014;13(10):1045-1060.

13 Liu SF, Gao X, Zhou SH. New target for prevention and treatment of neuroinflammation: microglia iron accumulation and ferroptosis. *ASN Neuro* 2022;14:17590914221133236.

14 Jia HR, Liu XL, Cao YY, *et al*. Deferoxamine ameliorates neurological dysfunction by inhibiting ferroptosis and neuroinflammation after traumatic brain injury. *Brain Res* 2023;1812:148383.

15 Yang S, Qi SN, Wang CG. The role of retinal Müller cells in diabetic retinopathy and related therapeutic advances. *Front Cell Dev Biol* 2022;10:1047487.

16 Walker RJ, Steinle JJ. Role of beta-adrenergic receptors in inflammatory marker expression in Müller cells. *Invest Ophthalmol Vis Sci* 2007;48(11):5276-5281.

17 Xu YJ, Jia BW, Li J, *et al*. The interplay between ferroptosis and neuroinflammation in central neurological disorders. *Antioxidants* (*Basel*) 2024;13(4):395.

18 Ndisang JF. Synergistic interaction between heme oxygenase (HO) and nuclear-factor E2- related factor-2 (Nrf2) against oxidative stress in cardiovascular related diseases. *Curr Pharm Des* 2017;23(10):1465-1470.

19 Komoto K, Nomoto T, El Muttaqien S, *et al*. Iron chelation cancer therapy using hydrophilic block copolymers conjugated with deferoxamine. *Cancer Sci* 2021;112(1):410-421.

20 Zhu DD, Liang RF, Liu Y, *et al*. Deferoxamine ameliorated $Al(mal)_3$-induced neuronal ferroptosis in adult rats by chelating brain iron to attenuate oxidative damage. *Toxicol Mech Meth* 2022;32(7):530-541.

21 Feng SQ, Yao X, Zhang Y, *et al*. Deferoxamine promotes recovery of traumatic spinal cord injury by inhibiting ferroptosis. *Neural Regen Res* 2019;14(3):532.

22 Sakamoto K, Suzuki T, Takahashi K, *et al*. Iron-chelating agents attenuate NMDA-Induced neuronal injury *via* reduction of oxidative stress in the rat retina. *Exp Eye Res* 2018;171:30-36.

23 Obolensky A, Berenshtein E, Lederman M, *et al*. Zinc-desferrioxamine attenuates retinal degeneration in the rd10 mouse model of retinitis pigmentosa. *Free Radic Biol Med* 2011;51(8):1482-1491.

24 Zhu MQ, Li N, Wang YN, *et al*. Regulation of inflammation by VEGF/BDNF signaling in mouse retinal Müller glial cells exposed to high glucose. *Cell Tissue Res* 2022;388(3):521-533.

25 Gong FY, Ge T, Liu J, *et al*. Trehalose inhibits ferroptosis *via* NRF2/HO-1 pathway and promotes functional recovery in mice with spinal cord injury. *Aging (Albany NY)* 2022;14(7):3216-3232.

26 Li HS, Lyu X, Rong A, *et al*. Vascular endothelial growth factor/connective tissue growth factor and proteomic analysis of aqueous humor after intravitreal conbercept for proliferative diabetes retinopathy. *Int J Ophthalmol* 2024;17(10):1816-1827.

27 Nag TC. Müller cell vulnerability in aging human retina: Implications on photoreceptor cell survival. *Exp Eye Res* 2023;235:109645.

28 Bringmann A, Pannicke T, Grosche J, *et al*. Müller cells in the healthy and diseased retina. *Prog Retin Eye Res* 2006;25(4):397-424.

29 Wang HQ, Wu S, Jiang XD, *et al*. Acteoside alleviates salsolinol-induced Parkinson's disease by inhibiting ferroptosis *via* activating Nrf2/SLC7A11/GPX4 pathway. *Exp Neurol* 2025;385:115084.

30 Cheng H, Wang PF, Wang N, *et al*. Neuroprotection of NRF2 against ferroptosis after traumatic brain injury in mice. *Antioxidants (Basel)* 2023;12(3):731.

31 Wang FF, Li R, Liao D, *et al*. Ghrelin alleviates high glucose-induced retinal microvascular endothelial cell injury by activating Nrf2/HO-1 pathway to inhibit ferroptosis. *Int J Ophthalmol* 2025;18(6):978-985.

32 Li Y, Ruan XH, Sun M, *et al*. Iron deposition participates in LPS-induced cognitive impairment by promoting neuroinflammation and ferroptosis in mice. *Exp Neurol* 2024;379:114862.

33 Zhang Y, He ML. Deferoxamine enhances alternative activation of microglia and inhibits amyloid beta deposits in APP/PS1 mice. *Brain Res* 2017;1677:86-92.

34 Stockwell BR, Friedmann Angeli JP, Bayir H, *et al*. Ferroptosis: a regulated cell death nexus linking metabolism, redox biology, and disease. *Cell* 2017;171(2):273-285.

35 Feng HZ, Stockwell BR. Unsolved mysteries: How does lipid peroxidation cause ferroptosis *PLoS Biol* 2018;16(5):e2006203.

36 Mandal PK, Seiler A, Perisic T, *et al*. System x(c)- and thioredoxin reductase 1 cooperatively rescue glutathione deficiency. *J Biol Chem* 2010;285(29):22244-22253.

37 Guo B, Phillips JD, Yu Y, *et al*. Iron regulates the intracellular degradation of iron regulatory protein 2 by the proteasome. *J Biol Chem* 1995;270(37):21645-21651.

38 Piñero DJ, Li N, Hu J, *et al*. The intracellular location of iron regulatory proteins is altered as a function of iron status in cell cultures and rat brain. *J Nutr* 2001;131(11):2831-2836.

39 Brewer AC, Murray TV, Arno M, *et al*. Nox4 regulates Nrf2 and glutathione redox in cardiomyocytes *in vivo*. *Free Radic Biol Med* 2011;51(1):205-215.

40 Akaishi R, Fujishima F, Ishida H, *et al*. Correlation between TXNRD1/HO-1 expression and response to neoadjuvant chemoradiation therapy in patients with esophageal squamous cell carcinoma. *Esophagus* 2022;19(3):436-443.

41 Chong CR, Chan WPA, Nguyen TH, *et al*. Thioredoxin-interacting protein: pathophysiology and emerging pharmacotherapeutics in cardiovascular disease and diabetes. *Cardiovasc Drugs Ther* 2014;28(4):347-360.

42 Chen W, Zhao MJ, Zhao SZ, *et al*. Activation of the TXNIP/NLRP3 inflammasome pathway contributes to inflammation in diabetic

retinopathy: a novel inhibitory effect of minocycline. *Inflamm Res* 2017;66(2):157-166.

43 Eissa LD, Ghobashy WA, El-Azab MF. Inhibition of thioredoxin-interacting protein and inflammasome assembly using verapamil mitigates diabetic retinopathy and pancreatic injury. *Eur J Pharmacol* 2021;901:174061.

44 Liu YP, Cui YF, Shi M, *et al*. Deferoxamine promotes MDA-MB-231 cell migration and invasion through increased ROS-dependent HIF-1α accumulation. *Cell Physiol Biochem* 2014;33(4): 1036-1046.

45 Corcoran SE, O'Neill LA. HIF1α and metabolic reprogramming in inflammation. *J Clin Invest* 2016;126(10):3699-3707.